High temperature materials for aerospace applications : Ni-based superalloys and γ-TiAl alloys

Mikael Perrut, Pierre Caron, Marc Thomas, Alain Couret

High temperature materials for aerospace applications : Ni-based superalloys and γ-TiAl alloys

Mikael Perrut[1], Pierre Caron[1], Marc Thomas[1], Alain Couret[2]

[1]Onera – The French Aerospace Lab, 92322, Châtillon, France
[2]CNRS, CEMES (Centre d'Elaboration de Matériaux et d'Etudes Structurales), BP 94347, 29 rue J. Marvig, 31055 Toulouse, France

Abstract

Two outstanding aerospace oriented high temperature materials, the single crystal nickel-based superalloys for high pressure turbine blades and the γ-TiAl based alloys for low pressure turbine blades, are being presented here. In both cases, the optimisation of their mechanical properties is based on a high knowledge of metallurgy, mixing together different aspects such as processes, alloy design, deformation mechanisms, impact of oxidative environment or interaction between protective layers and protected alloy. Historical evolutions are recalled and put into perspective with more recent research activities.

1/ General Introduction

Aeroengines need high temperature structural materials, namely for high pressure turbine (HPT), where Ni-based superalloys are unavoidable materials for the manufacturing of disks and blades. Their excellent mechanical properties, even under extreme conditions, come from their two-phased optimised microstructures that will be presented in detail. Long efforts of optimisation have been made concerning the metallurgical route, the thermal treatments, the chemical compositions and associated microstructures. Illustrations of these efforts will be given in the case of single crystal Ni-based superalloys. Some considerations about protective coatings will also be presented.

However, one drawback of these high temperature materials is their high density, typically between 8 and 9 $g.cm^{-3}$. Reducing the weight of turbine rotating components is very important for the reduction of engine energy consumption and greenhouse gases emissions. Substitute lighter materials have been sought for, especially in the low pressure turbine (LPT) where the conditions are not as extreme as in the HP turbine, one example being the γ-TiAl alloys. These intermetallic alloys have been first introduced in aeroengines in 2011 for the coldest LP turbine blades. Different processes have been studied for the optimisation of γ-TiAl alloys mechanical properties, some of these processes will be discussed along with the different generations of γ-TiAl alloys and their associated microstructures. However, some scientific points concerning these recent materials are not fully understood and we will focus on the aging of microstructures and mechanical properties which is a challenging problem to address.

2/ Nickel-based superalloys for single crystal turbine blades

2.1/ Introduction

Rotating and static blades in the high-pressure turbine section of aircraft and helicopter gas turbine engines are critical components as they experience a combination of very high temperatures, harsh and complex mechanical stresses and corrosive and oxidising environment. The concept of single crystal (SC) blades made of high-performance nickel-based superalloys was developed since the

1960's to contribute to the increase of the temperature capability of such components and to the lengthening of their life duration, thus improving the engine performances in terms of specific power, reduction of fuel consumption and cost of ownership.

Since the early 1980's, SC vanes and blades have been progressively introduced into the most advanced military and civil aircraft engines. These components are made of complex nickel-based superalloys containing significant amounts of refractory elements such as Mo, W, Ta and Re. The nickel-based face-centered-cubic γ matrix is strengthened by a high volume fraction, up to 70%, of ordered $L1_2$ γ'-Ni_3Al type precipitates.

The cast turbine blades were initially produced using conventional melting and casting processes and thus have a polycristalline equiaxed grain structure (Figure 2.1). However, high temperature creep under elevated centrifugal stress leads to cracking of grain boundaries normal to the principal stress axis that limits the life of the rotating blades. An intermediate step before the SC blade casting was the development of a directional solidification (DS) process producing columnar grain components in order to align the grain boundaries parallel to the main centrifugal stress direction, thus limiting, but not totally avoiding, grain boundary damages. A blade made of a single grain is the ultimate solution allowing to totally eliminate grain boundary cracking events. This evolution was allowed thanks to the development of a specific process of directional solidification including a grain selection system.

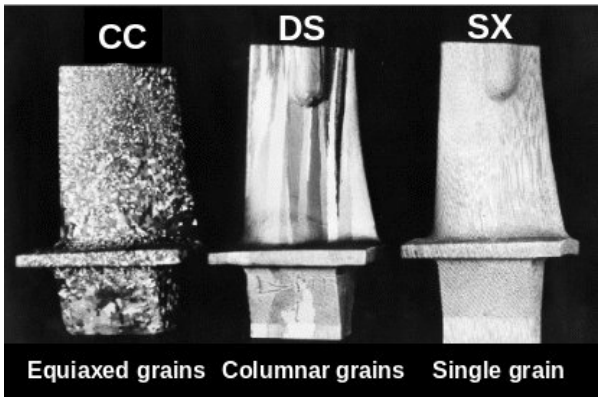

Figure 2.1 - As-cast high pressure turbine blades (courtesy Safran Helicopter Engines)

In parallel with the development of new casting processes, the chemistries of the nickel-based superalloys suited for SC blade applications continuously evolved by increasing progressively the contents of γ'-former elements such as Al, Ti and Ta, and thus the volume fraction of the γ'-strengthening phase, and by introducing higher amounts of solid solution refractory elements such as Mo, W, Ta, Re and possibly Ru.

The equiaxed grain and columnar grain blades are still used in the intermediate and low pressure sections of the gas turbines where the temperature is moderate or relatively low (around 600-900°C). However, the SC blades and vanes made of high-strength nickel-based superalloys are now inescapable in the high pressure section where the temperature experienced by these components may approach 1150°C in some circumstances.

2.2/ Microstructural and chemical features

The possibility to cast directionally solidified (DS) columnar grain, then single crystal (SC) superalloy blades was first demonstrated by Pratt & Withney Aircraft at the end of the 1960's [1]. The SC components are today produced using a lost wax investment casting process in Bridgman-type directional solidification furnaces. The molten metal is first poured into a multicomponent ceramic mold put down on a water-cooled chill plate. The temperature of the molten metal is about 200°C above the melting point of the alloy and solidification occurs through a temperature gradient

in the order of 40°C.cm^{-1} or less in the industrial furnaces. The mold is then vertically withdrawn from the furnace at a constant rate which is typically around 25 cm.h^{-1}. In the case of nickel-based superalloys the grains grow preferentially along a <001> type cristallographic orientation. To obtain a SC component, a grain selector is incorporated at the bottom of the mold just above a starter part, where columnar grain growth first occurs at the beginning of the solidification process. The grain selector may be a multiple-turn constriction of the mold or have a pig-tail (spiral) shape.

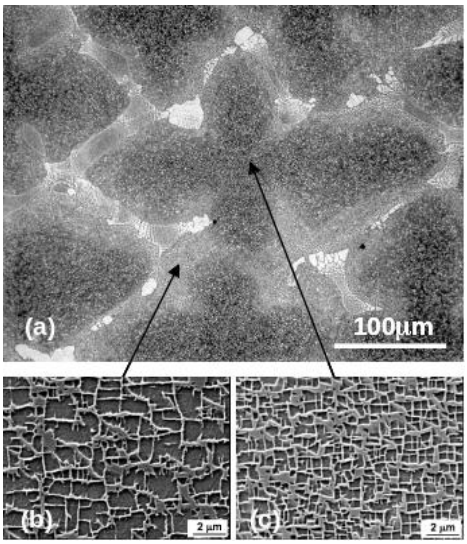

Figure 2.2 - Dendritic microstructure of the as-cast MC-NG SC superalloy normal to the <001> growth direction: (a) at the dendrite scale, imaged by light microscopy (LM); (b) and (c) γ' precipitates, imaged by scanning electron microscopy (SEM).

The conditions of solidification, withdrawal rate and thermal gradient, of the SC components lead to a dendritic structure with primary and secondary growth orientations along <001> directions. Figure 2.2 illustrates the as-cast dendritic structure of a MC-NG single crystal observed normally to the growth direction. The chemical etching reveals both chemical and microstructural variations in the transverse directions. Observations at a finer scale evidence a high volume fraction of γ' precipitates dispersed in the γ matrix within the dendrites. Their size increases from the center of the dendrites to the regions close to the coarse γ/γ' eutectic particles formed within the interdendritic areas at the end of the solidification process. A number of studies have been devoted to the homogenisation of this dendritic structure and to the optimisation of the size and distribution of the strengthening γ' precipitates. The seminal study of Jackson *et al*. has shown that the creep resistance of the γ'-strengthened nickel-based superalloys increased with the fraction of fine γ' precipitates [2]. High temperature homogenisation heat treatments are thus recommended to dissolve the coarse γ/γ' eutectic particles in order to benefit from a high amount of γ'-former elements for the further precipitation of the fine γ' particles. Thereafter, it was demonstrated that the size of the γ' precipitates can be controlled using adequate ageing heat treatments in order to optimise the mechanical strength of SC nickel-based superalloys, especially the creep strength.

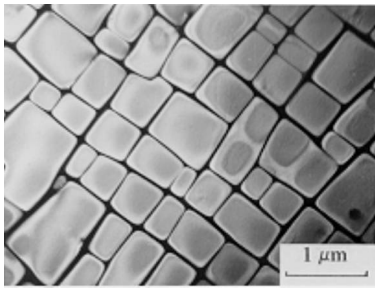

Figure 2.3 - Homogeneous distribution of γ' precipitates in fully heat-treated CMSX-2 SC superalloy (dark field TEM image).

Examples of chemistries of the different generations of nickel-based superalloys designed for SC blades are given in Table I. The first trials of SC castings were made using nickel-based superalloys initially designed for conventional or columnar grain castings. The following step was to design alloys derived from these polycristalline superalloys, but suited for SC casting mainly by suppressing the minor elements C, B, Hf and Zr which participate to the grain boundary strengthening, and then becoming obviously useless. A typical example is the NASAIR 100 SC alloy co-developed by NASA and Cannon-Muskegon Corp. [3] inspired by the Mar-M247 DS alloy. A huge benefit of suppressing volontary additions of minor elements was to significantly increase the incipient melting temperature and to allow the use of high temperature homogenisation heat treatments eliminating almost all the γ/γ' eutectic pools and solutioning all the γ' precipitates. After applying adequate solutioning and ageing heat treatment, the resulting microstructure is a homogeneous distribution of well-aligned cuboidal γ' precipitates with a mean size within the range 300-500 nm and a volume fraction up to 70% as obtained in the CMSX-2 SC superalloy (Figure 2.3). This major improvement paved the way for the development of new nickel-based superalloys specifically designed for SC applications. Since this time, the compositions of the SC nickel-based superalloys have continuously evolved with the aim of increasing their mechanical strength and temperature capability.

Table I : Typical chemistries of superalloys for single crystal components (wt. %)

Alloy	Ni	Co	Cr	Mo	Re	Ru	W	Al	Ti	Ta	Nb	Hf	C	B	Zr	Si
DS Mar-M247*	Base	10	8.3	0.7	-	-	10	5.5	1	3	-	1.4	0.15	0.015	0.05	-
NASAIR 100	Base	-	9	1	-	-	10.5	5.75	1.2	3.3	-	-	-	-	-	-
CSMX-2	Base	4.6	8	0.6	-	-	8	5.6	1	6	-	-	-	-	-	-
AM1	Base	6.5	7.8	2	-	-	5.7	5.2	1.1	7.9	-	-	-	-	-	-
CMSX-4	Base	9	6.5	0.6	3	-	6	5.6	1	6.5	-	0.1	-	-	-	-
CMSX-10	Base	3	2	0.4	6	-	5	5.7	0.2	8	0.1	0.03	-	-	-	-
MC544 (MC-NG)	Base	-	4	1	4	4	5	6	0.5	5	-	0.1	-	-	-	0.1
MC534	Base	-	4	4	5	4	3	5.8	-	6	-	0.1	-	-	-	0.1
TMS-162	Base	5.8	3	3.9	4.9	6	5.8	5.8	-	5.6	-	0.1	-	-	-	-
TMS-238	Base	6.5	5.8	1.1	6.4	5	4	5.9	-	7.6	0.1	-	-	-	-	-
CMSX-8	Base	10	5.4	0.6	1.5	-	8	5.7	0.7	8	-	0.2	-	-	-	-
CMSX-4 Plus	Base	10	3.5	0.6	4.8	-	6	5.7	0.85	8	-	0.1	-	-	-	-

** superalloy for columnar grain castings*

Whereas the first generation SC superalloys such as CMSX-2 [4] and AM1 [5] developed at the early 1980's contain the same major alloying elements, Co, Cr, Mo, W, Al, Ti and Ta, as in the previous nickel-based superalloys, the following generations all benefit from the addition of rhenium (Re) with contents up to 6.4 wt.%. Re acts as a very efficient solid solution strengthener of the γ matrix where this element partitions preferentially. As Re is characterised by a very low diffusion rate, it strongly reduces the kinetics of γ' precipitate coarsening at high temperatures that is beneficial to the mechanical properties. The diffusion controlled climb dislocation mechanisms active during creep at high temperature are also strongly slowed down due to Re addition. On the other hand, Re is a relatively rare and expensive material, that impacts negatively the cost of the alloy. The high molar mass of Re increases the density of the alloys, and a tight control of his content must be ensured in order to avoid casting defects such as freckles and precipitation of deleterious brittle topologically close-packed (TCP) phase precipitates, such as σ, μ and Laves phases. Despite these drawbacks, the second generation of SC nickel-based superalloys developed during the late 1980's and containing about 3 wt.% of Re, such as CMSX-4 [6] , PWA 1484 [7] and René N5 [8], are now widely used in civil and military engines, and even in industrial land based gas turbine engines for electric power generation. The success of these alloys inspired the

development of third generation SC nickel-based superalloys during the 1990's, such as CMSX-10 [9] and René N6 [10], containing around 6 wt.% of Re. These alloys are however scarcely used as the drawbacks due to their high level of Re become too penalizing to allow their extensive industrialisation.

Addition of ruthenium (Ru) in the fourth generation SC nickel-based superalloys such as MC-NG (MC544) [11], MX-4 (EPM-102) [12], TMS-138 [13] around the 2000's was an attempt to counteract the deleterious effects of Re additions. Alloys containing both additions of Re and Ru make them effectively less prone to precipitation of deleterious TCP phase and lighter than high-Re materials. These promising results have even encouraged the recent development at the NIMS (National Institute for Materials Science, Japan) of fifth and sixth generation SC nickel-based superalloys containing high levels of both Re and Ru, such as TMS-162 [14] and TMS-238 [15], respectively. However as Ru is even more rare and expensive than Re, the engine manufacturers still strongly hesitate to choose such alloys for industrial use of single crystal blades and vanes. The tendency today is to carefully adjust the level of Re taking into account the proper specifications of each type of engine in terms of cost and performances. One solution proposed is to decrease the level of Re at a value intermediate between the first and second generation alloys, as in the CMSX-8 alloy where the Re content is 1.5 wt.% [16]. The most recent developments concern alloys with level of Re between those of second and third generation alloys, such an example being the CMSX-4 Plus alloy containing 4.8 wt.% of Re [17].

2.3/ Mechanical behaviour

As creep strength is of utmost importance for the rotating blades, the main part of the studies devoted to the mechanical behaviour of SC superalloys are concentrated on the influence of chemistry and microstructure on the creep behaviour of these materials. The study of the creep behaviour of SC superalloys along the <001> orientation of the blade is of prime importance as it corresponds to the centrifugal loading direction. However attention is also focused on the mechanical behaviour of SC superalloys along other cristallographic orientations, such as <111> and <011>. It is indeed needed to evaluate the effects of anisotropy and the response of these materials under multi-axial stresses generated locally due to the complex shape of the blade root and platform and in some cases, because of the intricate cooling schemes in the airfoil section.

As a typical example, the study of the creep behaviour at 760°C and 750 MPa of the SC CMSX-2 superalloy revealed spectacular cross effects of γ' precipitate size and tensile axis orientation [18]. This temperature is typically of concern for the platform and the bottom part of the airfoil. As the creep life along <001> increases when the γ' precipitate size goes from 230 to 450 nm, the effect is inverse along <111> (Figure 2.4). In the <001> single crystals containing the largest precipitates, the deformation operates mainly by homogeneous a/2<110>{111} multiple slip in the γ matrix channels, leading to rapid formation of dense dislocation networks at the γ/γ' interfaces, promoting efficient strain hardening, a limited extent of primary creep and a long stress-rupture life. Surprisingly, despite that <111> is a multiple slip orientation (six equally stressed a/2<110>{111} slip systems), the primary creep deformation operated mainly by coplanar slip in the primary slip plane in near-<111> oriented crept specimens. Absence of secondary creep indicates that the first activated slip system remains predominant throughout their entire life, resulting in weak strain hardening, high creep rate and poor creep strength. Reducing the γ' size to 230 nm promotes extensive cooperative shearing of the γ/γ' structure by <112>{111} slip in both <001> and <111> SC specimens with the creation of superlattice intrinsic and extrinsic stacking faults (SISF and SESF) within the γ' precipitates. The planar character of this mode of deformation promotes heterogeneous deformation for both orientations but the lower <112>{111} Schmid Factor for <111> than for <001> (respectively 0.31 and 0.47) explains the lower creep rate and the higher creep strength exhibited by the <111> specimens.

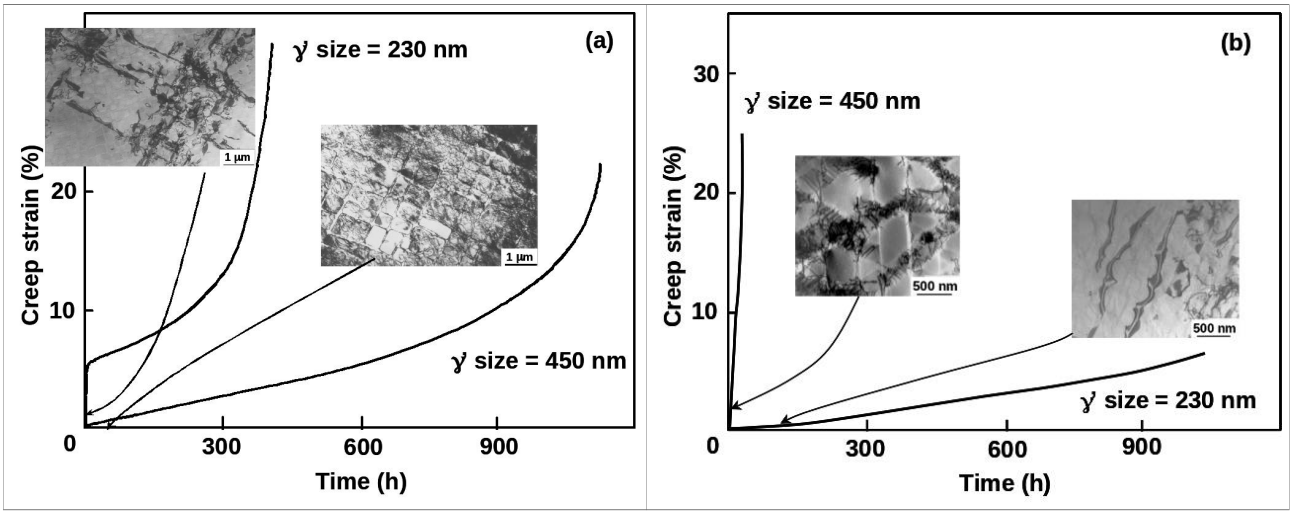

Figure 2.4 - Effect of the γ' precipitate size on the deformation mechanisms and creep behaviour at 760°C and 750 MPa of CMSX-2 SC superalloy along: a) <001>; b) <111>.

For a given precipitate size, the creep behaviour at 760°C along <001> also strongly depends on the alloy chemistry which determines some particular features such as levels of solid solution strengthening and stacking fault energy of both γ and γ' phases, and amplitude of the mismatch between the lattice parameters of γ and γ' phases (the γ/γ' mismatch is defined as $\delta = 2(a_{\gamma'} - a_{\gamma})/(a_{\gamma'} + a_{\gamma})$, where $a_{\gamma'}$ and a_{γ} are the lattice parameters of the γ' and γ phases respectively). This is illustrated in Figure 2.5 by comparing the creep behaviours at 760°C and 840 MPa of two fourth generation SC superalloys MC544 (MC-NG) and MC534 [19]. The γ' size was fixed at 310 nm in both alloys with a γ' volume fraction around 70% that determines the same Orowan stress in the γ matrix channels of both alloys. The main difference between both alloys is the maximum value of the γ/γ' mismatch of -4.4 x 10^{-3} and -14.2 x 10^{-3} in MC544 and MC534, respectively. The creep behaviour of MC544 is characterised by a high amplitude of primary creep and a relatively short creep life, whereas the primary creep amplitude is weak for MC534 and the creep life very long.

Analyses of the dislocation structures revealed that the matrix dislocations are confined within the γ channels in the MC534 alloy, forming dense dislocation networks at the γ/γ' interfaces. The high creep resistance of MC534 is associated to the very low primary creep amplitude, itself related to the homogeneous character of the deformation which promotes an efficient strain hardening. The high level of misfit coherency stress in MC534 promotes spreading of the matrix dislocations in the narrow horizontal γ matrix channels by a/2<110>{111} slip, instead of shearing of the γ' precipitates thus leading to rapid strain hardening. The decorrelated movement of Shockley partials in the vertical matrix channels, with creation of a number of stacking faults, signs the difficulty for perfect matrix dislocations to move between the γ' precipitates. On the other hand, the large primary creep extent and the resulting poor creep resistance of MC544 characterised by a much lower value of mismatch is linked to the heterogeneous character of the deformation resulting from the shearing of the γ' particles by extensive <112>{111} slip.

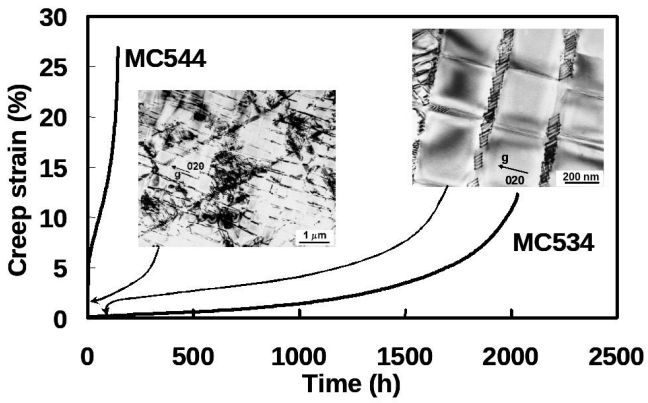

Figure 2.5 - Creep behaviour and deformation mechanisms at 760°C and 840 MPa of MC544 and MC534 <001> single crystal specimens.

A huge number of studies are also dedicated to the creep behaviour of SC superalloys at high temperatures, typically above 900°C, concerning the airfoil part of the blade. A special attention is generally paid to the specific phenomenon of oriented coalescence of the γ' precipitates leading to the formation of the so-called γ/γ' rafted microstructure, which influences the creep behaviour itself, but also the tensile and fatigue behaviour of the SC superalloys.

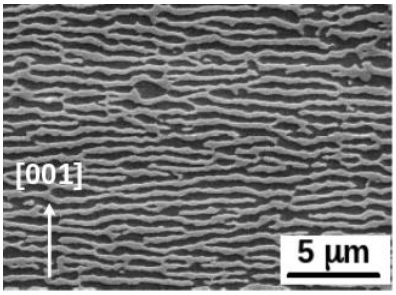

Figure 2.6 - γ/γ' rafted microstructure in AM1 SC superalloy after 20 hours of tensile creep along [001] at 1050°C and 150 MPa (SEM; longitudinal section; γ' phase in dark).

During creep of commercial nickel-based single crystal superalloys at temperatures above 900°C and under <001> tensile loading, combined effects of centrifugal stress, diffusion, γ/γ' coherency stress and γ/γ' elastic modulus misfit cause directional coalescence of strengthening γ' precipitates as rafts perpendicular to the tensile axis (Figure 2.6). The quasi-stationary secondary creep stage typically observed during creep at 1050°C of SC superalloys is associated to the stability of this rafted microstructure where deformation occurs mainly by a combination of slip and climb mechanisms of a/2<110> matrix dislocations leading to the formation of dense and regular dislocations networks at the γ/γ' interfaces. As early mentioned by Fredholm and Strudel in the experimental SC superalloy 221 [20], the destabilisation of the rafted microstructure during the creep life at 1050°C occurs through a topological inversion of the γ/γ' microstructure which causes the progressive increase of the creep rate. The γ' precipitates are initially finely dispersed in the γ matrix which is the connected phase. When the γ' precipitates coalesce during the primary creep stage to form the γ' rafts, the γ' phase is still the connected phase but afterwards, the γ/γ' rafted microstructure can indeed progressively evolve such as the γ' phase completely surrounds γ phase particles. This topological inversion coincides with the onset of the accelerated creep stage which is linked to a growing activity of the deformation mechanisms in both γ and γ' phases. Analysis of this phenomenon in various SC superalloys shows that topological inversion occurs in superalloys where the γ' phase fraction is higher than about 50% and therefore depends on the alloy chemistry and on the temperature [21]. The γ/γ' topological inversion occurs as earlier as the γ' fraction is higher.

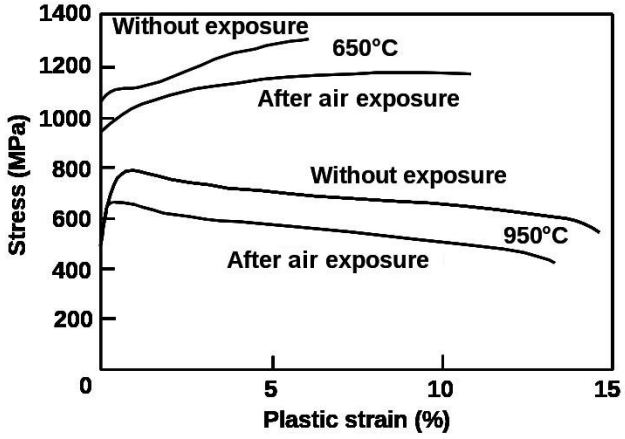

Figure 2.7 - Effect of an air exposure for 200 hours at 1050°C and 80 MPa on the engineering stress-strain tensile curves at 650°C and 950°C of <001> MC2 single crystals.

Formation of the rafted structure also influences the tensile behaviour of the SC superalloys by modifying the elemental deformation mechanisms. As an example, the tensile strength at 650°C and 950°C of the MC2 SC superalloy with a rafted γ/γ' microstructure, produced by a preliminary ageing treatment in air at 1050°C during 200 hours under a tensile stress of 80 MPa, is significantly lower than that of the alloy containing a homogeneous distribution of cuboidal γ' precipitates with a mean size of 400 nm (Figure 2.7) [22]. The decrease in tensile stress for the aged material is associated with the coalescence of the γ' precipitates which facilitates the Orowan by-passing mechanism of the precipitates by a/2<110> matrix dislocations.

As compared with polycristalline superalloys, the SC superalloys are also characterised by a higher resistance to low cycle fatigue and thermal fatigue thanks to the minimum Young modulus value along the preferential <001> stress axis that induces lower stress for a given imposed strain. Moreover, the absence of carbides retards crack initiation which principally occurs at interdendritic casting pores. The high level of yield strength at high temperatures also participate to the high fatigue resistance of SC superalloys that contributes to the lengthening of the life duration of SC superalloys components, especially in the case of cooled blades and vanes which are subjected to severe thermal fatigue stresses.

2.4/ Interactions with protective coatings

When designing new chemistries of SC superalloys, the increase of the mechanical strength at high temperatures is favoured to the detriment of the oxidation and corrosion resistance, mainly due to a continuous decrease of their Cr content. The SC blades therefore need to be protected by specific alloy coatings with a high intrinsic resistance to environment. Moreover, the most advanced SC cooled blades are protected by an external thermal barrier coating (TBC) based on a porous ceramic that reduces the temperature of the superalloy substrate. The main types of protective alloy coatings are aluminide diffusion coatings, typically β-NiAl based intermetallic coatings, and metallic overlay coatings of the composition MCrAlY (M = Ni, Co or a mixture of both elements). A typical thermal barrier composition is $Zr_2O_3/8\%Y_2O_3$ deposited using a Electron Beam Phase Vapor Deposition (EB-PVD) process. When a TBC is applied, aluminide and MCrAlY coatings are used as bond coats in between the alloy substrate and the external ceramic coating.

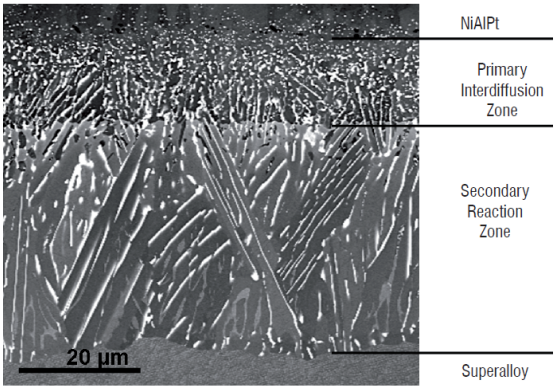

Figure 2.8 - Microstructure of the diffusion zone in as-coated MC544 SC (longitudinal section; SEM).

A major issue for coated SC nickel-based superalloys is the chemical interactions between the superalloy substrate and the coating, occuring during the coating process and, later, in service at high temperatures. The interdiffusion phenomena can indeed lead to more or less important chemical and microstructural modifications of both materials that may have deleterious effects on the mechanical behaviour of the substrate. As an example, in coated first and second generation SC

nickel-based superalloys protected by a Pt-modified nickel aluminide bond coat, interdiffusion phenomena modify the superalloy beneath the coating by creating a primary interdiffusion zone with a β-NiAl(Pt) matrix, this zone containing precipitates rich in refractory elements. In third and fourth generation alloys, a deeper secondary reaction zone (SRZ) may develop in the alloy under the primary diffusion zone as in the MC-NG alloy protected by a NiAl(Pt) bondcoat (Figure 28) [23]. The recrystallised SRZ microstructure is cellular with a γ' phase matrix containing elongated γ particles and intermetallic TCP phase precipitates. The driving forces for SRZ formation are the local changes of composition due to aluminium diffusion towards the superalloy and diffusion of nickel and refractory alloying elements in the opposite direction. Residual stress resulting from the alloy surface preparation prior to coating also contribute to the SRZ formation. Due to its specific microstructure, the mechanical strength of the SRZ is inferred to be significantly lower than that of the γ/γ' substrate. Formation of SRZ thus causes a reduction of the load bearing section of the superalloy component which impacts negatively its creep and fatigue strength. Moreover, the polycristalline structure of the SRZ promotes propagation of intergranular microcracks which initiate in the brittle NiAl coating. During creep of coated MC-NG, it has been demonstrated that the stress-rupture life at 1050°C is reduced compared to the bare alloy, due to the formation of the primary and secondary interdiffusion zone, whose total depth reaches 140 µm after 199 hours of creep [23]. However, if microcraks are observed within the SRZ, they never propagate in the superalloy substrate. On the other hand, during low cycle fatigue (LCF) tests at 650°C of coated MC-NG superalloy specimens, the decrease of the fatigue strength as compared to the bare superalloy cannot been explained solely by the reduction of load bearing section due to the SRZ formation. Actually, cracks start in the brittle NiAlPt layer, then follow the grain boundaries within the SRZ and propagate within the superalloy (Figure 2.9), that explains the resulting loss of LCF strength [23].

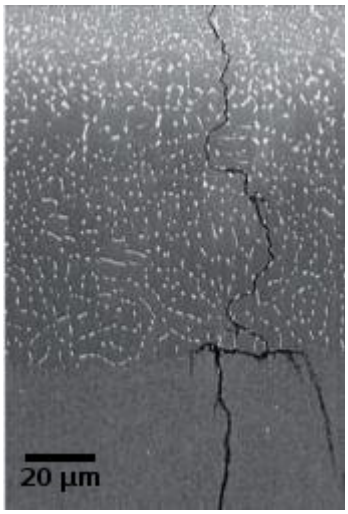

Figure 2.9 - Propagation of a crack through the SRZ and the γ/γ' structure of a NiAlPt coated MC544 SC specimen failed during LCF at 650°C (longitudinal section; SEM).

In order to avoid or, at less, to minimize the formation of SRZ, the alloy substrate chemistry must therefore be adapted to the bond coat. Analysis of the results obtained for various superalloys coated with a platinum modified NiAl coating thus reveals that the presence of rhenium is necessary, but not sufficient, for SRZ development [24]. On the contrary, cobalt is inferred to play an inhibitive role. The major teachings are that when designing new superalloys for single crystal blades which must be coated, a supplementary criterion must be the absence of proneness to SRZ formation under the coating, in order to avoid deleterious effects on mechanical properties and thus on the blade life.

It has been also demonstrated that the the life of the ceramic coating depends on the chemistry of the superalloy substrate. Interdiffusion phenomena induce changes of chemistry and mechanical strength of the bondcoat, but also of the thin Al_2O_3 oxide layer which forms at the interface between the bond coat and the ceramic top coat. An increase of the creep strength of the bondcoat alloy thus

reduces rumpling at the bond coat/ceramic interface which in turn retards the spallation of the ceramic coating. For instance Ti and Co are thus inferred to have a deleterious effect on the TBC life, whereas additions of minor elements such as Hf, Y or La improve the adherence of the ceramic coating.

2.5/ Research and industrial applications in France

Studies on DS and SC superalloys, including casting of single crystal samples and components, started in France at the end of the 1960's, particularly at Snecma (today Safran Aircraft Engines), School of Mines of Paris and Onera. A joint programme for the development of new materials (PDNM) started at the end of 1970's in order to design French nickel-based superalloys for SC blades and vanes for the benefit of the new aircraft and helicopter engines of Snecma and Turbomeca (today Safran Helicopter Engines). The AM1 superalloy was thus jointly developed by Snecma, School of Mines, Imphy S.A. and Onera, in the first place to be introduced as high pressure gas turbine blade and vane material in the M88 engine powering the military RAFALE fighter. Since this time, the AM1 alloy was also introduced in the TP400-D6 engine (Europrop International consortium between Snecma, Rolls-Royce, ITP and MTU) powering the Airbus A400M military transport aircraft and in the SaM146 engine (joint venture of Snecma and NPO Saturn) powering the Sukhoi Superjet 100 regional aircraft. Meanwhile, the low density AM3 [25] and high creep strength MC2 [26] superalloys were designed at Onera and then introduced by Turbomeca in several helicopter engines such as ARRIUS 2 and ARRIEL 2.

Continuation of alloy development activities at Onera during the 1990's led to the design of the fourth generation MC-NG superalloy for aircraft turbine blades and of the THYMONEL 8 superalloy for rocket engine turbopumps, with a low susceptibility to hydrogen embrittlement [27]. The SCB444 and SCA425 nickel-based superalloys designed for use in land-based gas turbines for power generation were also developed in the frame of a European research programme in partnership with ONERA, ALSTOM, Turbomeca, HOWMET, EDF and the Hahn-Meitner-Institut in Berlin [28]. These alloys exhibit a good balance between long-term creep properties and high temperature corrosion resistance in the harsh environment of industrial gas turbines.

Along with the alloy development activities, research programmes were undertaken in numerous university laboratories in France in order to contribute to the understanding of the various mechanisms controlling the behaviour of the SC superalloys. During the 1980-1990's, three successive research programmes were conducted within the frame of University scientific groups dedicated to single crystal superalloys with the financial support of Ministry of Defence and CNRS, and in collaboration with Snecma, Turbomeca, Onera, and School of Mines of Paris [29-31]. During the 2000's, specific research activities were undertaken at ENSMA and CIRIMAT, focusing on the very high temperature creep behaviour of SC superalloys and on the creep behaviour of coated materials. Numerous PhD theses were thus conducted in the universities of Grenoble, Nancy, Paris, Poitiers, Rouen, Toulouse, allowing to provide a huge and deep knowledge of the elemental mechanisms controlling the microstructural evolutions and the various mechanical behaviours of this particular class of materials.

2.6/ Conclusions and perspectives

The technology of SC blades is today widely introduced in the aeronautical and industrial gas turbines. If design of new alloys is still an activity which get SC superalloys specialist worked-up, patents being still regularly applied every year, identification of original superalloy compositions for SC casting becomes more and more difficult. At the beginning, the main objective was to get a stress-rupture life as long as possible. The challenge today is more complex, looking to obtain the best balance between several properties including low sensitivity to casting defects, moderate cost and density, weak interactions with the protective coatings, good microstructural stability, high creep strength in a wide range of temperatures, fatigue strength and thermal fatigue strength. It

remains therefore some possibility to design the SC superalloy chemistry for a given blade application which keeps the way open for a few improvements as regards as the temperature capability, the life, the compatibility with the protective coatings, the cost reduction. From a more academical point of view, the optimisation of the efficiency and life of the system superalloy/bond coat/thermal barrier still needs a better understanding of the mechanisms controlling the interactions between the different layers. Another issue, that is not addressed in this paper, is the development of efficient and reliable models allowing to predict the SC component life, taking into account the in-service microstructural evolution of the superalloys and the impact of the protective coatings.

3/ Titanium Aluminides for Low Pressure Turbine Blades

3.1/ Introduction

Regarding environmental issues, the civil air transport industry is subjected to regulations of noise and chemical pollution emanating from the International Civil Aviation Organization (ICAO), but is also highly dependent on oil resources which become scarcer while switching to other energy sources remains problematic. ICAO regulations, which always evolve towards greater severity, are preparing for the coming years new standards that incorporate other pollutants, such as soot aerosols and carbon dioxide (CO_2) while strictly limiting NOx emissions and noise pollution. Therefore, the motorists in charge of aeroengine development strive to optimize existing systems. Along with improved emission control, the problem of life components in the engines depends on the ability of these components to withstand thermomechanical stresses that can be applied in operational conditions. Therefore, there is still a strong need to develop technological advances involving high-performance materials in terms of thermal and mechanical properties, in order to achieve drastic weight gain with a favourable impact on fuel consumption, polluting emissions and noise.

In this context, TiAl alloys, exhibiting a density twice lower (~ 4 g/cm^3) than that of nickel-based superalloys (~ 8 g/cm^3), are considered to be really attractive for high temperature applications owing to their high specific modulus and mechanical strength and to a very good oxidation resistance (Figure 3.1) [32,33]. This is the reason why extensive efforts were devoted worldwide to the development of such intermetallic materials for the last thirty years. The present paper will be focused on TiAl technological breakthroughs in France over the last ten years.

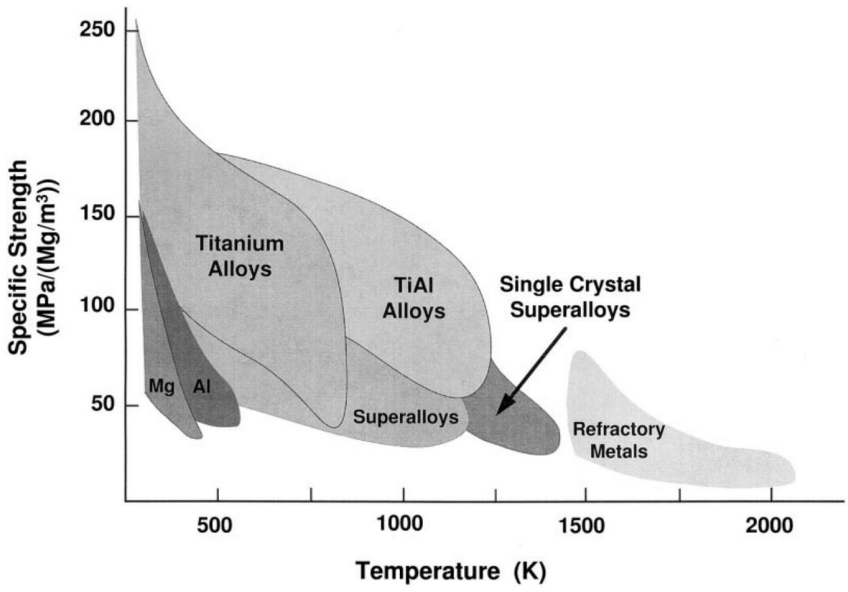

Figure 3.1 - Temperature capabilities of different classes of materials.

3.2/ TiAl-based blades for aeroengines

The story starts in 2007 when General Electric (GE) announced that their patented Ti-48Al-2Cr-2Nb (at%) alloy will be implemented in the low pressure turbine (LPT) for their new GEnX engine. This announcement immediately lead to a high level of R&D activities in different countries. However, the manufacturing of the GE blades was far to be cost-effective. Indeed, such TiAl blades were produced by investment casting, a manufacturing process which i) inherently generates property variability for different thickness of the cast parts, ii) requires extensive machining and iii) leads to limited properties in terms of strength and ductility [34-36]. The inherent lack of strength is associated with the coarse cast structure. It is important to note that cast processing is mostly limited by the fact that optimized microstructures are difficult to achieve. Attempts were made to modify the columnar cast structure and to reduce cast segregations through heat treatments, but with limited success. The end-user was then inclined to adopt a microstructure of compromise, the so-called duplex microstructure, which is composed of both γ grains and $\gamma+\alpha_2$ lamellar colonies. Cast LPT blades using the Ti-48Al-2Cr-2Nb (at%) alloy with the aforementioned duplex microstructure have been introduced in the GEnX engines in 2011, and the same blades are currently being produced by means of investment casting. Nowadays, centrifugal casting appears to be the mature technology for a better control of potential cast-induced defects and this technology was introduced for the manufacture of Ti-48Al-2Cr-2Nb turbine blades in the CFM LEAP engine in 2016 (Figure 3.2). However, the cast Ti-48Al-2Cr-2Nb alloy being limited to the lower pressure stage (700°C), tremendous work has been done in terms of microstructure optimisation and alloy design to extend the service temperature up to 800-850°C, while guaranteeing a proper balance of desired properties.

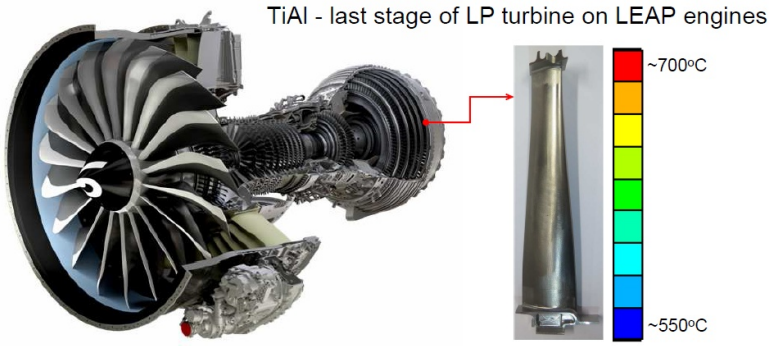

Figure 3.2 - CFM LEAP engine and location of the γ-TiAl based blades in the turbine.

At this stage, it should be pointed out that the mechanical properties in γ-TiAl alloys are strongly governed by the microstructure, which in turn is affected by the chosen processing route. Therefore, a strict control of mechanical properties is achieved only by optimising the microstructure over different length scales, which means the knowledge of the size, morphology, fraction and distribution of the constitutive phases. For a successful use in the turbine part of aircraft engines, TiAl-based alloys should exhibit a reasonable ductility at room temperature (more than 1%) and an elevated strength at the service temperature (700-800°C). Now, the Ti-48Al-2Cr-2Nb (at%) alloy is solidified through the L+β→ α peritectic reaction. Under further cooling, the phase transformation is referred to the α (hcp) → α_2 (DO_{19}) + γ ($L1_0$) reaction, where nucleation and growth of γ lamellae with the Blackburn relationship is followed by α → α_2 ordering. The growth of these γ lamellae inside the α grains lead to the very specific lamellar structure of TiAl-based alloys. Then, subsequent heat treatments can be used to develop various microstructures such as near γ, duplex (lamellar structure mixed with single-phased γ grains), near lamellar or even fully-lamellar ones. These microstructures can be modified by incursion in the high temperature β phase field in alloys with low aluminum content and/or containing β stabilizers [37-39]. While most of the alloy design work is devoted to low aluminum alloys for wrought applications, namely in Germany and Japan, another strategy is possible by selecting aluminum-rich alloys for their higher oxidation resistance

and their better creep resistance compared to low aluminium content alloys. Furthermore, refractory elements which are generally strong β stabilizers are candidates for improved creep resistance.

Among the different generic TiAl-based alloys microstructures, one may satisfy industrial requirements. Specifically, fine microstructures with grains smaller than a few tenths of micrometers, and predominantly containing lamellar structure, are known to offer a good compromise in mechanical properties [40]. However, it is difficult to obtain such fine lamellar microstructures by using conventional cast processing. On the other hand, such optimised microstructures can be achieved by Powder Metallurgy (PM) which generates inherently non textured and homogeneous structures. In the last decade, extensive in-house work has been concentrated on the microstructure – mechanical property relationships for the PM Ti-48Al-2Cr-2Nb (at%) alloy, and also for other (more advanced) chemical compositions. However, PM processing requires a strict control of the powder quality. During atomization, gas-induced porosities are easily entrapped in the powder particles that are, in addition, surface contaminated due to the high reactivity of the TiAl alloys with oxygen.

In parallel to German teams who developed PM Metal Injection Moulding (MIM) for producing turbine blades, two alternative rapid processings have been used in France for TiAl alloys to refine the microstructures: the novel technique called Spark Plasma Sintering (SPS) was developed at CEMES and the Laser Metal Deposition (LMD) technique was investigated mainly at ONERA.

3.3/ Rapid processings

First of all, Spark Plasma Sintering (SPS) is actually an emerging PM technique, which is original due to the heating method of the sample: heating is performed by applying a direct pulsed current of high intensity (Figure 3.3) [41,42]. In this process, the powder, being encapsulated in a graphite assembly, is submitted to an uniaxial pressure by two punches that also transmit the electrical power to the sample. For conducting materials such as TiAl-based alloys, rapid heating occurs mainly by Joule's effect and full densification is achieved in a relatively short time. Due to the limited solid state diffusion, fine and metastable microstructures with enhanced properties can be achieved. Thus, this process was assumed to be a good candidate to reach desirable fine equiaxed lamellar microstructures. In order to satisfy the double compromise between, on the one hand, properties at room temperature and high temperatures, and, on the other hand, between strength and ductility, a fine equiaxed lamellar microstructure was developed with a hardened γ phase and a predominance of lamellar colonies. Furthermore, thermal-induced inhomogeneities were successfully reduced by adding a small quantity of boron for grain impingement, thanks to a grain boundary pinning mechanism by TiB_2 precipitates. Accordingly, fine-grained fully lamellar microstructures can be tailored by careful control of minor additions of boron without subsequent heat treatment. Moreover, the same uniform microstructure can be maintained for a large sintering temperature interval, i.e. 1190-1250°C (Figure 3.4). This is an interesting result for the purpose of complex shaping of γ-TiAl blades, which consist in a slim foil and a thick root with different local thermal conditions.

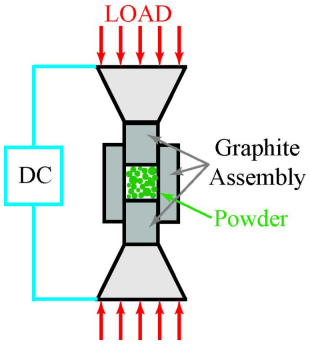

Figure 3.3 - Schematic set-up of the SPS technology.

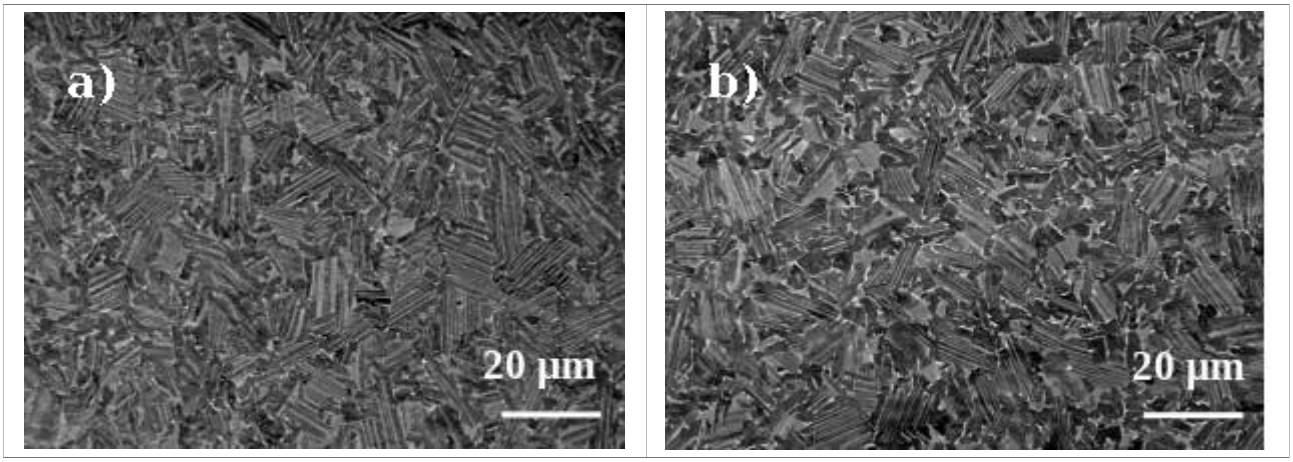

Figure 3.4 - Fine-grained fully lamellar microstructures obtained for a) SPS at 1190°C, b) SPS at 1250°C.

Within the framework of the ANR IRIS project [43], near net-shaping of TiAl turbine blades have been developed by the SPS technique. A specific assembly has been designed to limit the temperature heterogeneity, to avoid any failure of the graphite parts under the applied load and to absorb any withdrawal during cooling [44]. The punches have been divided into several parts of different lengths to fully densify both the root and the foil. With such an inherent simplicity of the process, this one-step technology appears to be cost effective and therefore represents a breakthrough in the use of TiAl-based alloys to improve efficiency of aeroengines. In this project, a tungsten-containing alloy, named IRIS, was developed to optimise high temperature properties. The addition of a refractory element such as tungsten was chosen to enhance creep resistance by reducing the mobility of dislocations, actually moving through a climb mechanism involving diffusion [45]. The near lamellar microstructure of this IRIS alloy consists of refined lamellar colonies of approximately 30 µm. These lamellar colonies are surrounded by γ borders that expand laterally over a few micrometers (Figure 3.5). The γ borders originate from a remaining β phase surrounding the α grains from temperatures above the α transus. This high temperature β phase helps to limit the grain growth, in addition to the boron effect. It subsequently transforms into γ + B2 during cooling, leading to the observed microstructure of the borders. The IRIS microstructure yields a very long creep life of more than 4000 hours at 700°C under 300 MPa, which is comparable to the most competitive existing TiAl alloys. Moreover, the combination of high strength at low and high temperatures is achieved owing to different mechanisms, i.e. the strengthening of the γ phase due to the high level of tungsten atoms, the limited size of γ borders and the predominance of the lamellar microstructure. The good ductility is attributed to the deformability of γ borders but also to the deformability of lamellar colonies (due to their low volume fraction of α_2 phase). Besides, the limited grain size is known to avoid the formation of long dislocation pile-ups, which could be sources of stress concentrations leading to the sample failure.

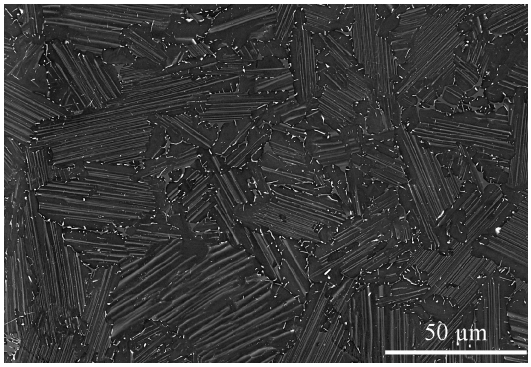

Figure 3.5 - Typical microstructure of the IRIS alloy ; the borders of the lamellar colonies are composed of black γ phase and white B2 phase.

The second novel technique to be presented here is an additive manufacturing process called Laser Metal Deposition (LMD). This technique consists in injecting a powder through a nozzle onto the substrate, and melting this powder layer by layer. This direct processing is attractive compared to SPS since it requires no hard tooling. A CAD file is used to index the laser and the powder supply which is aimed at building 3D parts. High power density is used for this process, thus leading to very high cooling rates of the order of 10^3 up to 10^4 °C.s^{-1}, resulting in ultra-fine and metastable structures. On the other hand, these high thermal gradients tend to build up residual stresses, which is rather challenging for a high crack sensitivity material such as TiAl.

Collaborative work between the ENSAM ParisTech and ONERA was performed to evaluate the feasibility to produce sound LMD parts using the Ti-48Al-2Cr-2Nb (at%) alloy. It has been demonstrated that uncracked samples can be achieved by optimising the most influent parameters (laser power, powder feeding rate, displacement rate) and by using different laser sources to reduce thermal gradients. Firstly, the substrate was pre-heated at a temperature of 300°C. Secondly, the laser provided in-situ local melting to diminish thermal gradients in the deposited TiAl-based material. Thirdly, a second laser source with a lower energy density was set up to yield gradual post-heating in order to slow down the cooling rate and relieve the residual stresses [46]. A better dilution and a better coupling with the substrate were ensured by concomitantly reducing the feeding rate and increasing the laser power. Post-heat treatments were carried out for stress relaxation and structural homogenisation purposes. A sub-transus solution annealing at 1250°C provided an interesting duplex microstructure. This microstructure was selected for tensile testings, which were very encouraging. It was actually shown that crack-free test samples were obtained with a good tensile ductility (~ 1 to 2 % of total elongation), which is equivalent to or even better than the ductility of the same material in a traditional cast + HIP route. The post-heat treatments were also successful to restore the structural homogeneity and to relieve the residual stresses.

3.3/ Environmental effects

The last topic to be presented deals with the environmental-related property degradation for TiAl-based alloys. One of the most challenging issues of the last ten years was to assess the mechanical performance of γ-TiAl alloys after long-term exposure at potential service temperatures. Indeed, a number of investigations have reported a significant reduction in ductility which occurs after exposure at service temperatures such as 650-700°C. The reason for this is apparently not specific to one alloy in particular, although some factors may be composition-dependent. First, it was found that the ductility can be restored by removing the outer layer of test specimens, suggesting a surface oxidation problem [47]. However, exposure at 700°C under vacuum leads to the same embrittlement which may also be indicative of a residual stress dependence on the ductility loss [48]. Some additional causes have been identified in the literature for this material embrittlement: structural instabilities [49,50], more in-depth interstitial contaminations [51,52], hydrogen and moisture embrittlement [53-56], aluminium depletion [57-59], formation of brittle phase particles [48,60], nitrogen effect [61].

Accordingly, attempts were made at ONERA to identify the prevailing factors of this material embrittlement by using a careful procedure to separate mutual effects between environmental and non-environmental factors [62]. For this investigation, a pre-alloyed Ti-48Al-2Cr-2Nb (at%) alloy was densified by HIP at 1200°C for 4 hours and 140 MPa. In the as-HIPed condition, the near-γ microstructure consisted in γ grains with a mean size of 9 μm and a very low volume fraction of secondary α_2 phase (~1%). In the as-received (as-HIPed) condition, the machining procedures (grinding finish, grinding + electro-polishing, turning + electro-polishing) have been compared for residual stress purpose by using room temperature tensile tests. We have observed that tensile results did not show any significant effect of the machining procedure despite different residual stress distributions, since electro-polishing allows to remove compressive residual stresses from grinding. In addition, the good ductility for the electro-polishing finish was not related to a better surface roughness since fracture proceeded internally. Further insights about the deformation

mechanisms revealed that mechanical twinning occurs through the entire gage length of the test sample and that the motion of ordinary dislocations are progressively hindered by the new twinning interfaces, thus leading to the build-up of dislocation tangles. In the case of the electro-polished test samples, the surface exhibits some deformation features that can be ascribed to mechanical twinning (Figure 3.6). Interestingly, cross twinning at the surface does not appear to induce any micro-cracks which might lead to the premature failure of the test sample.

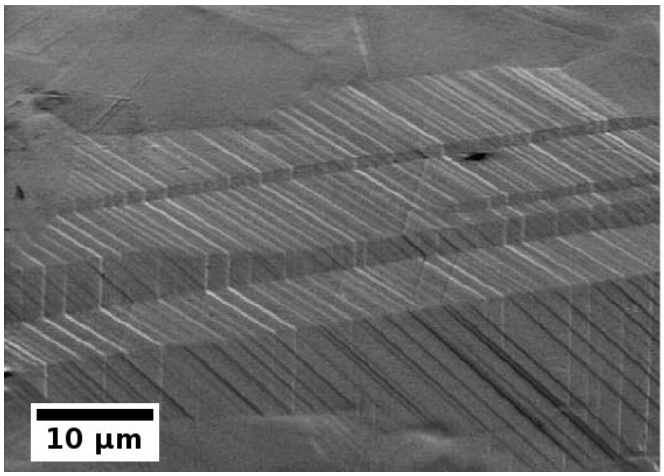

Figure 3.6 - Typical cross twinning at the surface of the polished test sample.

The deformation mechanisms for this near γ-microstructure were clearly identified, but the effect of a long-term exposure had to be questioned. Annealing at 700°C for 400 hours in ambient air resulted in a strong embrittlement of all test samples, with tensile elongation values down to 0.1 - 0.5% irrespective of the machining procedure. However, when blanks were first exposed at 700°C for 400 hours and then machined, the tensile properties do not differ much from the as-received condition. The differences in tensile ductility between surface-removed and surface-retained samples are definitely ascribed to a surface-related embrittlement, as confirmed by the fact that the surface-retained samples actually failed from the surface. SEM observations revealed that a 1-2 µm thick oxide scale did form. Moreover, an Al-depletion layer together with 0.2 µm precipitates, probably Nb-rich according to the BSE contrast, have also been detected below the oxide scale. Therefore, cracking could be expected either at the oxide-Ti_3Al interface or at the surface, and should therefore intervene rapidly during loading.

Another interesting question was the determination of the minimum duration at 700°C that might affect properties. For this purpose, a short exposure of 2 hours at 700°C was investigated. A less severe detrimental effect on ductility was obtained for this annealing time of 2 hours with respect to 400 hours, with strain values between 0.2 and 0.9%. Since no oxide layer was detected at the surface for such a short duration, a more in-depth contamination by interstitial species was assumed. In order to identify a possible oxygen penetration and diffusion inside the material, microhardness profiles were measured as a function of depth from the surface. However, no measurable effect of interstitial penetration was detected. For this reason, ductility loss after exposure at 700°C for 2 hours still remains unclear, whereas for longer duration, the formation of an oxide scale with related sub-scales has definitely a detrimental effect.

In another respect, it is interesting to note that the stress-strain curves reveal that all the 700°C exposed test samples failed during the “plateau” regime, i.e. during twinning propagation. Polished fracture surface as well as electro-polished gage length surface were used to determine the mechanisms involved in the fracture. Mechanical twinning was not evidenced at the surface, suggesting that a twinning arrest mechanism may occur in the upper layer. This means that deformation is not accommodated at the surface, which results in the build-up of stress concentrations in the sub-scale. In addition, the fact that the test samples were air-cooled may generate an additional residual stress gradient from the outer part towards the inner part of the

sample. Finally, this surface-related embrittlement was confirmed by undertaking a mechanical polishing of 10 µm after short term-exposure, which lead to recover tensile ductility. In this case, the fracture expertise showed that the rupture occurs far from the surface, similarly as the as-received material.

As a conclusion, the embrittlement mechanism appears to be microstructure-dependent since a positive effect of heat treatment prior to machining was observed. For instance, for a nearly lamellar microstructure, obtained after sub-transus annealing at 1340°C for 10 hours, a homogeneous deformation is known to take place by dislocation slip and twinning through the numerous obstacles of lamellae interfaces. Now, after short term exposure at 700°C, it is interesting to point out that room temperature tensile properties remain unaffected for this sub-transus microstructure. Hence, the susceptibility to environmental embrittlement can be reduced by using heat treatments at a temperature high enough, so to have a significant amount of lamellar microstructure, which may prevent extensive mechanical twinning. A lower cooling rate is also recommended for residual stress purpose.

3.4/ Conclusions

Concerning γ-TiAl alloys, a better consistency in mechanical properties was successfully achieved by using prealloyed powder metallurgy (PM). Indeed, PM appears to be successful to promote sufficient grain refinement and to ensure a good structural homogeneity, thus leading to low property variability. Moreover, powder compacts produced by SPS display very attractive mechanical properties at room temperature in terms of strength and ductility. SPS can then be considered as a viable manufacturing route by demonstrating that near net-shaping of TiAl blades is possible and that balanced mechanical properties at room temperature and high temperatures can be achieved, in a single run and without subsequent thermal treatment. Furthermore, the feasibility of applying laser forming to the manufacture of γ-TiAl parts has been evaluated on the basis of a good geometrical quality, a satisfying metallurgical integrity and the possibility to achieve an optimised microstructure. Finally, some environmental and non-environmental factors have been identified to be prevalent on the TiAl-based alloys embrittlement. The facts that crack initiation site features are present in the sub-scale close to the surface in the case of exposed samples and that the removal of the surface layer after exposure enables to restore the initial ductility, can account for a surface-related embrittlement during exposure. Several factors were found to play a role in the ductility loss after short term exposure, such as an oxygen-enriched surface, a mechanical twinning propagation that is hindered towards the surface, and a residual stress gradient generated by air cooling.

4/ General conclusions

Two different high temperature aerospace materials classes were presented. On the one hand, it has been shown that the single crystal nickel-based superalloys still undergo improvements, namely through the research of multi-criteria optimisation, including efficiency of the whole system superalloy/bond coat/ thermal barrier. On the other hand, titanium aluminides have not the same technology readiness level, being much newer to industrial use in aeroengines. New processes, such as Spark Plasma Sintering, may help to develop long-term viable manufacturing route for a new generation of TiAl blades, while surface effects and associated embrittlement should definitely be studied more in detail in the next years.

5/ References

[1] F. L. Versnyder, M. E. Shank, "The Development of Columnar Grain and Single Crystal High Temperature Materials Through Directional Solidification", *Mater. Sci. Eng.* **6** (1970) 213-247.

[2] J.J. Jackson, M.J. Donachie, R.J. Henricks, M. Gell, “The Effect of Volume Percent of Fine γ’ on Creep in DS Mar-M200 + Hf”, *Met. Trans. A* **8A** (1977) 1616-1620.

[3] T.E. Strangman, G.S. Hoppin III, C.M. Phipps, K. Harris, R.E. Schwer, "Development of exothermically cast single-crystal Mar-M247 and derivative alloys", Superalloys 1980, J.K. Tien *et al*. eds, ASM, Metals Park, OH, USA, 1980, pp. 215-224.

[4] K. Harris, G.L. Erickson, R.E. Schwer, "Mar M 247 derivations – CM 247 LC DS alloy, CMSX single crystal alloys, properties and performance”, Superalloys 1984, M. Gell *et al*. eds, The Metallurgical Society of AIME, Warrendale, PA, USA, 1984, pp. 221–230.

[5] J.H. Davidson, A. Fredholm, T. Khan, J.-M. Théret, French patent N° 2 557 598, 1983.

[6] K. Harris, G.L. Erickson, R.E. Schwer, D.J. Frasier, J.R. Whetstone, "Process and alloy optimization for CMSX-4 superalloy single crystal airfoils", High Temperature Materials for Power Engineering 1990, Part II, E. Bachelet *et al*. eds., Kluwer Academic Publishers, Dordrecht, Holland, 1990, pp. 1281–1300.

[7] A.D. Cetel, D.N. Duhl, "Second-generation nickel-base single crystal superalloy", Superalloys 1988, D.N. Duhl *et al*. eds., The Metallurgical Society, Inc., Warrendale, PA, USA, 1988, pp. 235–244.

[8] C.S. Wukusick, L. Buchakjian, Jr., Patent Application #GB 2 235 697 A, March 1991.

[9] G.L. Erickson, "The development and application of CMSX-10", Superalloys 1996, R.D. Kissinger *et al*. eds., The Minerals, Metals & Materials Society,Warrendale, PA, USA, 1996, pp. 35–44.

[10] W.S. Walston, K.S. O’Hara, E.W. Ross, T.M. Pollock, W.H. Murphy, "René N6: third generation single crystal superalloy”, Superalloys 1996, R.D. Kissinger *et al*. eds., The Minerals, Metals & Materials Society, Warrendale, PA, USA, 1996, pp. 27–34.

[11] P. Caron, “High γ’ solvus new generation nickel-based superalloys for single crystal turbine blade applications”, Superalloys 2000, T.M. Pollock *et al*. eds., TMS, Warrendale, PA, USA, 2000, pp. 737-746.

[12] S. Walston, A. Cetel, R. MacKay, K.O’Hara, D. Duhl and R. Dreshfield, "Joint development of a fourth generation single crystal superalloy", Superalloys 2004, K.A. Green *et al*. eds., TMS, Warrendale, PA, USA, 2004, pp. 15-24.

[13] J.X. Zhang, T. Murakamo, Y. Koizumi, T. Kobayashi, H. Harada, S. Masaki, Jr., "Interfacial dislocation networks strengthening a fourth-generation single-crystal TMS-138 superalloy", Metall. Mater.Trans. A **33**A (2002), p. 3741-3746.

[14] A. Sato, H. Harada, A.-C. Yeh, K. Kawagishi, T. Kobayashi, Y. Koizumi, T. Yokokawa, J.X. Zhang, "A 5th generation SC superalloy with balanced high temperature properties and processability", Superalloy 2008, R.C. Reed *et al*. eds, TMS, Warrendale, PA, USA, 2008, pp. 131-138.

[15] K.Kawagishi, A.-C. Yeh, T. Yokokawa, T. Kobayashi, Y. Koizumi, H. Harada, "Development of an oxidation-resistant high-strength sixth-generation single-crystal superalloy TMS-238", Superalloys 2012, E.S. Huron *et al*., eds, John Wiley & Sons, Inc., Hoboken, New Jersey, USA, 2012, pp. 189-195.

[16] J.B. Wahl, K. Harris, "New single crystal superalloys, CMSX®-7 and CMSX®-8", Superalloys 2012, E.S. Huron *et al*., eds, John Wiley & Sons, Inc., Hoboken, New Jersey, USA, 2012, pp. 179-188.

[17] J.B. Wahl, K. Harris, "CMSX-4® Plus single crystal alloy development, characterization and application development", Superalloys 2016, M. Hardy *et al*., eds., John Wiley & Sons, Inc., Hoboken, New Jersey, USA, 2016, pp. 25-33.

[18] P. Caron, Y. Ohta, Y.G. Nakagawa, T. Khan, "Creep Deformation Anisotropy in Single Crystal Superalloys", Superalloys 1988, D.N. Duhl *et al*. eds., The Metallurgical Society, Inc., Warrendale, PA, USA, 1988, pp. 215-224.

[19] P. Caron, F. Diologent, "Effect of the γ/γ' lattice mismatch on the creep behaviour at 760°C of new generation single crystal superalloys", TMS 2008 Annual Meeting Supplemental Proceedings, Volume 3: General Paper Selections, TMS, Warrendale, USA (2008), 171-176.

[20] A. Fredholm, J.-L. Strudel, "High temperature creep mechanisms in single crystals of some high performance nickel base superalloys," High temperature Alloys, their Exploitable Potential, Proceedings of the Petten International Conference, J.B. Mariott *et al*. eds, Elsevier Applied Science, London, U.K., 1987, pp. 9-18.

[21] P. Caron, C. Ramusat, F. Diologent, "Influence of the γ' fraction on the γ/γ' topological inversion during high temperature creep of single crystal superalloys", Superalloys 2008, R.C. Reed *et al*. eds., TMS, Warrendale, PA, USA (2008) pp. 159-167.

[22] M. Pessah-Simonetti, P. Caron, T. Khan, "Effect of a long-term prior aging on the tensile behaviour of a high performance single crystal superalloy", *Journal de Physique IV* Colloque C7, supplement to the Journal de Physique 111, Volume 3, November 1993, pp. 347-350.

[23] O. Lavigne, C. Ramusat, S. Drawin, P. Caron, D. Boivin, J.-L. Pouchou, "Relationships between microstructural instabilities and mechanical behaviour in new generation nickel-based single crystal superalloys", Superalloys 2004, K.A. Green *et al*. eds., TMS, Warrendale, PA, USA, 2004, pp. 667-675.

[24] P. Caron, O. Lavigne, C. Ramusat, J. Benoist, C. Rio, "Secondary reaction zones in coated single crystal superalloy", Superalloys and Coatings for High Temperature Applications, TMS Annual Meeting 2005, San Francisco, CA, USA, 13-17 February 2005.

[25] T. Khan, "Recent developments and potential of single crystal superalloys for advanced turbine blades", High Temperature Alloys for Gas Turbines and Other Applications 1986, W. Betz *et al*. eds., D. Reidel Publishing Company, Dordrecht, Holland, 1986, pp. 21-50.

[26] P. Caron, T. Khan, "Development of a new nickel based single crystal turbine blade alloy for very high temperatures", *Advanced Materials and Processes*, Vol. 1, H.E. Exner, V. Schumacher, eds., DGM Informationsgesellschaft mbH, Oberursel, Germany, 1990, pp. 333–338.

[27] P. Caron, D. Cornu, T. Khan, J.-M. De Monicault, "Development of a Hydrogen Resistant Superalloy for Single Crystal Blade Application in Rocket Engine Turbopump", Superalloys 1996, R.D. Kissinger *et al*. eds., The Minerals, Metals & Materials Society, Warrendale, PA, U.S.A.,1996, pp. 53-60.

[28] P. Caron, A. Escalé, G. McColvin, M. Blackler, R. Wahi, L. Lelait, "Development of new high strength corrosion resistant single crystal superalloys for industrial gas turbine applications",

PARSONS 2000 - Advanced Materials for 21st Century Turbines and Power Plant, A. Strang *et al*. eds., IOM Communications Ltd, London, UK, 2000, pp. 847-864.

[29] Actes du Colloque National Superalliages Monocristallins, Villard-de-Lans, France. 26-28 February 1986.

[30] Actes du Colloque National Superalliages Monocristallins, Nancy, France, 22-23 November 1990.

[31] Comptes rendus du Colloque Superalliage Monocristallins, Toulouse-Seilh, France, 22-24 March 1995.

[32] Y-W. Kim, and D.M. Dimiduk, JOM **43**-8 (1991) pp. 40-47.

[33] W. Smarsly, H. Baur, G. Glitz, H. Clemens, T. Khan and M. Thomas, In: Hemker KJ, Dimiduk DM, Clemens H, Darolia R, Inui H, Larsen JM, Sikka VK, Thomas M, Whittenberger JD, editors. Structural Intermetallics 2001, Warrendale, PA, TMS, 2001, pp. 25-34.

[34] J.D.H. Paul, *et al.,* "Strength properties of a precipitation hardened high niobium containing Titanium aluminides alloy", In: Gamma Titanium Aluminides Edited by Y.W. Kim, H. Clemens & A.H. Rosenberger - TMS 2003 (2003) pp. 403-408 .

[35] M. Thomas, J.L. Raviart and F. Popoff, "Cast and PM processing development in gamma aluminides", *Intermetallics* **13** (2005) pp. 944-951 .

[36] X. Wu, "Review of alloy and process development of TiAl alloys", *Intermetallics* **14** (2006) pp. 1114-1122.

[37] Y. Yamamoto and M. Takeyama, "Physical metallurgy of single crystal gamma titanium aluminide alloys: orientation control and thermal stability of lamellar microstructure", *Intermetallics* **13** (2005) pp. 965-970.

[38] M. Grange, J.L. Raviart, and M. Thomas, "Influence of Microstructure on Tensile and Creep Properties of a New Castable TiAl-Based Alloy", *Metallurgical and Materials Transaction A* **354** (2004) pp. 2087-2102 .

[39] H. Clemens, *et al., "*Design of novel beta-solidifying TiAl alloys with adjustable beta/B2-phase fraction and excellent hot-workability", *Advanced Engineering Materials* **10** (2008) pp. 707-713.

[40] Y-W. Kim, "Effects of microstructure on the deformation and fracture of γ-TiAl alloys", *Materials Sciences and Engineering* **A192** (1995) pp. 519-533.

[41] A. Couret, *et al.,* "Microstructures and mechanical properties of TiAl alloys consolidated by spark plasma sintering", *Intermetallics* **16** (2008) pp. 1134-1141.

[42] R. Orru*, et al.,* "Consolidation/synthesis of materials by electric current activated/assisted sintering", *Materials Sciences and Engineering* **R63** (2009) pp. 127-287.

[43] Innovative manufacturing Route for Intermetallic alloys by spark plasma net Shaping (IRIS), project funded by the Agence Nationale de la Recherche (ANR), scientific coordinator O. Martin (MECACHROME), 2009-2012.

[44] A. Couret, *et al.,* Procédé de fabrication par frittage flash d'une pièce métallique de forme

complexe, Patent n°PCT/IB2012/051527 (2012).

[45] J.P. Monchoux and A. Couret, A microscopic study of the creep of a cast TiAl alloy at 750° C under 150 MPa, *Scripta Materiala* 65 (2011) pp. 198-201.

[46] M. Thomas. T. Malot and P. Aubry, 'Laser Metal Deposition of the Intermetallic TiAl Alloy', *Met. Trans. A*, **48**-6 (2017) pp.3143-3158.

[47] S.L. Draper, B.A. Lerch, I.E. Locci, M. Shazly, V. Prakash, *Intermetallics* **13** (2005) pp.1014-19.

[48] R. Pather, W.A. Mitten, P. Holdway, H.S. Ubhi, A. Wisbey, J.W. Brooks, *Intermetallics* **11** (2003) pp. 1015-27.

[49] Z.W. Huang, W. Voyce, W.P. Bowen, In: J.K. Hemker, D.M. Dimiduk, H. Clemens, R. Darolia, H. Inui, J.M. Larsen, V.K. Sikka, M. Thomas, J.D. Whittenberger, eds. Structural Intermetallics 2001, Warrendale, PA, TMS, 2001, pp. 551-60.

[50] M. Beschliesser, H. Clemens, H. Kestler, F. Jeglitsch, *Scripta Mater* **49** (2003) pp. 279-84.

[51] Y.W. Kim, In: Stiegler JO et al, eds. High Temperature Ordered Intermetallic Alloys IV, MRS, 1991, pp. 777-94.

[52] T. Kawabata, M. Tadano, O. Izumi. *Scripta Met* **22** (1988) pp. 1725.

[53] C.T. Liu, Y.W. Kim, *Scripta Met* **27**-5 (1992) pp. 599-603.

[54] T.J. Kelly, C.M. Austin, P.J. Fink, J. Schaeffer, *Scripta Metall et Mater* **30**-9 (1994) pp.1105-10.

[55] A.M. Brass, J. Chêne, *J. Mater Sci and Eng* **A272** (1999) pp. 269-78.

[56] A. Zeller, F. Dettenwanger, M. Schütze, *Intermetallics* **10** (2002) pp. 59-72.

[57] S.L. Draper, G. Das, I. Locci, J.D. Whittenberger, B.A. Lerch, H. Kestler, In: Y.W. Kim, H. Clemens, A.H. Rosenberger, eds. Gamma Titanium Aluminides 2003, Warrendale, PA, TMS, 2003, pp.207-12.

[58] X.Y. Li, S. Taniguchi, *Intermetallics* **13**-7 (2005) pp. 683-93.

[59] V. Maurice, G. Despert, S. Zanna, P. Josso, M.P. Bacos, P. Marcus, *Surf Sci* **596**-1/2 (2005) pp. 61.

[60] G. Schumacher, F. Dettenwanger, M. Schütze, A. Iberl, D. Reil, *Oxid. of Met.* **54**-3/4 (2000) pp. 317-37.

[61] F. Dettenwanger, E. Schumann, M. Rühle, J. Rakowski, G.H. Meier, *Oxid. of Met.* **50**-3/4 (1998) pp. 269-305.

[62] M. Thomas, O. Berteaux, F. Popoff, M.P. Bacos, A. Morel, B. Passilly, V. Ji, *Intermetallics* **14** (2006) pp. 1143-1150.